Monte Carlo calculations in comparison to neutron scattering studies: 3. On the structure of 12-arm star molecules

Klaus Huber, Walther Burchard, Siegfried Bantle* and Lewis J. Fetters†
Institute of Macromolecular Chemistry, University of Freiburg, D-7800 Freiburg, FRG
(Received 29 October 1986; revised 25 March 1987; accepted 19 June 1987)

The small-angle neutron scattering curves of polystyrene 12-arm star molecules exhibit deviations from the Gaussian star model according to Benoit. These deviations are comparable with those observed in the scattering curves of simulated polymethylene 12-arm star chains. They can be partially interpreted in terms of chain stiffness within the arms. If the simulated chains contain a specific star centre, their scattering curves, normalized by the radius of gyration, are in good agreement with the normalized experimental scattering curves. For very short arms the scattering curves of the simulated chains with a specific star centre approach the particle scattering factor of the rod-like star model.

(Keywords: SANS; 12-arm star molecules; chain stiffness; Monte Carlo simulations; star centre influence; particle scattering factor)

INTRODUCTION

In the preceding paper[1], the global dimensions of polystyrene (PS) regular 12-arm-star molecules and of simulated polymethylene (PM) 12-arm star chains were investigated. In the present paper, we would like to extend the comprehension of the structure of the same regularly branched 12-arm star molecules by considering the full angular dependence of the particle scattering factor $P(q)$. Here q is the scattering vector, defined as:

$$q = 4\pi/\lambda \sin(\theta/2) \quad (1)$$

where θ is the scattering angle and λ is the wavelength in the medium. To obtain the scattering behaviour, we performed small-angle neutron scattering (SANS) experiments over a wide q-range ($0 < q < 3.6\,\mathrm{nm}^{-1}$).

The only existing analytical theory on the scatter-ing behaviour of star molecules is based on a model, in which the segment–segment distances follow Gaussian statistics[2-4]. This model is based on a pure combination of linear chains and does not take into account the effect of a realistic star centre. In order to expand the theoretical picture of star branched molecules, we calculated the particle scattering factors of the other limiting model, where linear rods are linked together under special angles, forming the star-arms. We expected this special star to be a good model for a star centre.

First, the theory, based on the Gaussian model, was compared with our SANS curves. To find a detailed interpretation of the observed discrepancies between theory and experiment, we carried out Monte Carlo simulations of (PM) 12-arm star chains on the basis of Flory's rotational isomeric state (r.i.s.) model[5]. Two different methods were used in linking together the arms to a star. A detailed description of both methods was given in the preceding paper[1].

In the one method the star chains were simulated using two arms which were connected at the star centre. The star properties were then calculated using a special weighting procedure for inter-arm and intra-arm pair combinations of scattering centres. These simulated molecules were termed the 'combinatorial star'. This method is implicitly applied in the 'Gaussian' star model[2,6]. In the other method a special star centre was used that consists of four rigid sub-chains each of them containing five bonds. The conformation of these sub-chains was chosen such that the ends lie on the edges of a tetrahedron and form the junction points for three further arms. A comparison of the results derived by the two methods should yield the net effect of an extended star centre on the particle scattering factor. These Monte Carlo simulations do not account for excluded volume effects in the sense of 'self-avoiding walks'; they only show how the scattering behaviour is influenced by a star centre with fixed angles between the arms. With the stretched sub-chains in the star centre, excluded volume is nevertheless implicitly included to some extent.

This behaviour was also generated by calculation of the particle scattering factors for the 'hedgehog' model with rod-like arms. The main feature of this model is the correlation between the directions of the arms, which should occur in a realistic star centre.

EXPERIMENTAL

The SANS measurements reported in this paper were carried out with two different PS 12-arm star samples both in toluene-d_8 and cyclohexane-d_{12}. They are identical to PS 9–12 and PS 4–12 of the previous papers[1,7]. All experiments were performed at the Institut Max von Laue–Paul Langevin (ILL), Grenoble, France. The Monte Carlo simulations were performed with a Sperry Univac 1100/81 configuration at the computational centre of the University of Freiburg. For each

* Institut Laue-Langevin, Grenoble, France; present address: Sandoz AG, Basle, Switzerland.
† Present address: Corporate Research–Science Laboratories, Exxon Research and Engineering Co., Annandale, NJ 08801, USA

0032-3861/87/121997-07$03.00

star chain at least 1000 different conformations were generated. Details of the SANS experiments as well as of the computer simulations were described in refs. 1 and 8.

SANS EXPERIMENTS IN CYCLOHEXANE-D_{12}

As was shown by Burchard[4], a plot of $P(q) \times q^2 \rightarrow q$, (Kratky plot), is particularly sensitive to branching. In the case of regularly branched stars, this plot exhibits a characteristic maximum, followed by a plateau region. If the normalized version of this plot is used with

$$u = q\langle S^2 \rangle^{1/2} \tag{2}$$

where $\langle S^2 \rangle^{1/2}$ is the radius of gyration, the height $[P(u) \times u^2]_{max}$ and the position u_{max} of this maximum is only a function of the number of arms f. In the following, we used Kratky-plots to represent the scattering behaviour of star molecules.

The position of the maximum in the normalized Kratky-plot is determined by the following equation

$$V = \frac{2[V - 1 + \exp(-V) + (f+1)/2(1-\exp(-V))^2]}{1 - \exp(-V)[1 - (f-1)(1-\exp(-V))]} \tag{3}$$

with

$$V = u_{max} f/(3f-2) \tag{4}$$

For $f = 12$, one finds $u_{max} = 2.07$ and $[P(u)u^2]_{max} = 1.27$. Also the height of the final plateau is fixed by f. With a decreasing number of arms, the plateau is increased and if $f \leq 3$, i.e. for 3-arm stars and linear chains, the maximum disappears completely.

In a recent paper, Khorramian and Stivala[9] applied Burchard's[4] method on small-angle X-ray scattering curves of PS 12-arm star molecules in methyl-ethyl-ketone at 25°C to determine the number of arms f. The PS samples used therein are in part identical to those used in refs. 1 and 7. In this section, we discuss the scattering experiments with the sample PS 9–12 at $T = 28$°C and with PS 4–12 at $T = 35$°C in cyclohexane-d_{12}, a θ-solvent.

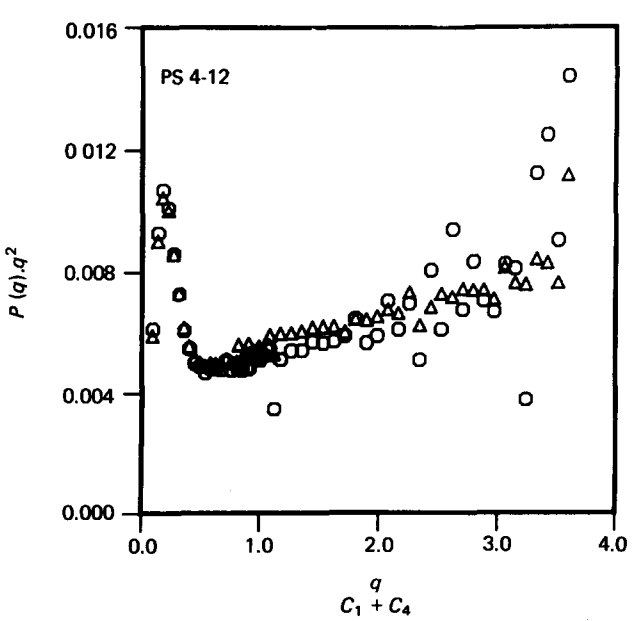

Figure 1 PS 4–12 in cyclohexane-d_{12} at $T = 35$°C; Kratky-plots of the scattering curves at c_1 (○) and c_4 (△)

Table 1 Concentration dependence of $\langle S^2 \rangle^{1/2}$ received from an analysis of the SANS data in the low q-range according to Berry[10]

Sample	c	c ($g\,cm^{-3}$)	$\langle S^2 \rangle^{1/2}$ (nm)
PS 9–12[a]	c_1	0.0249	3.40
$M_w = 55000$	c_2	0.0306	3.27
	c_3	0.0350	3.24
PS 4–12[b]	c_1	0.00235	11.67
$M_w = 467000$	c_2	0.00395	11.66
	c_3	0.00655	11.90
	c_4	0.00785	11.58

[a] Measurements at $T = 28$°C
[b] Measurements at $T = 35$°C

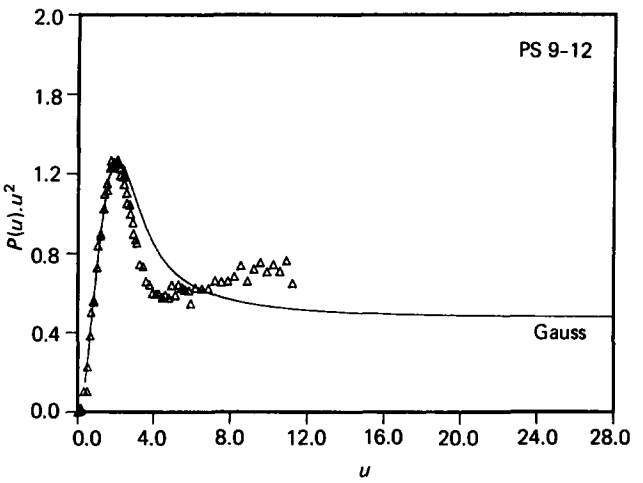

Figure 2 Normalized Kratky-plots under θ-conditions: comparison between the particle scattering factors of PS 9–12 at c_1 ($u = q \times 3.65$ nm) and the Gaussian star model[2]

In both cases the particle scattering factors were independent of concentration and could therefore be used directly for a comparison with theory and Monte Carlo simulations. *Figure 1* represents as an example the particle scattering factors of PS 4–12 at two different concentrations.

To normalize the scattering curves, the $\langle S^2 \rangle_z$ values derived from Berry-plots[10,11], i.e. from the initial part of the q-dependent square root reciprocal scattering intensity can be used. Results of these square root plots are collected in *Table 1*. Alternatively, we adjusted the experimentally found maximum height to the theoretically predicted one. This procedure is justified since it can be assumed that the theoretical expression is a good approximation to the experiment if $u \leq u_{max}$.

Figures 2 and *3* are representations of SANS scattering curves of concentration c_1 both from PS 9–12 and PS 4–12. Normalization was performed by adjusting the experimental maximum height to the theoretically predicted one, based on the Gaussian model. As can be seen from both Figures, theory and experiment merge with each other up to u_{max} and the resultant $\langle S^2 \rangle^{1/2}$ values, 3.65 nm (PS 9–12) and 10.97 nm (PS 4–12) are in fair agreement with those of *Table 1*.

At $u > u_{max}$ significant deviations from the theoretical curve occur, which are more pronounced for the sample with the lower molecular weight (PS 9–12). First there is a steeper descent than predicted by the theory[2]; then the curve passes through a minimum and does not lead into the characteristic plateau, but increases continuously. A quantitative interpretation has not been feasible so far.

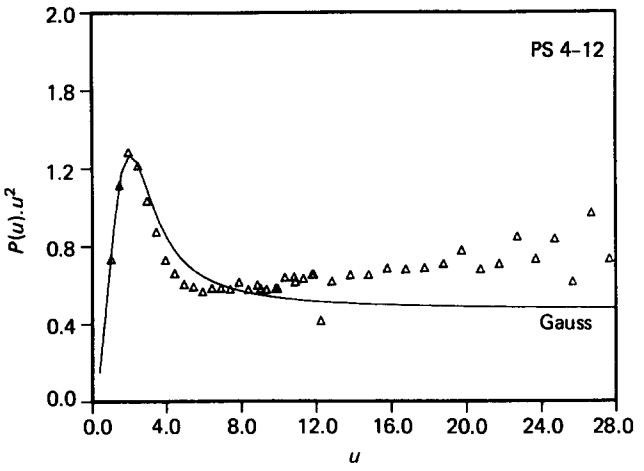

Figure 3 Normalized Kratky-plots under θ-conditions: comparison between the particle scattering factors of PS 4–12 at c_1 ($u = q \times 10.97$ nm) and the Gaussian star model[2]

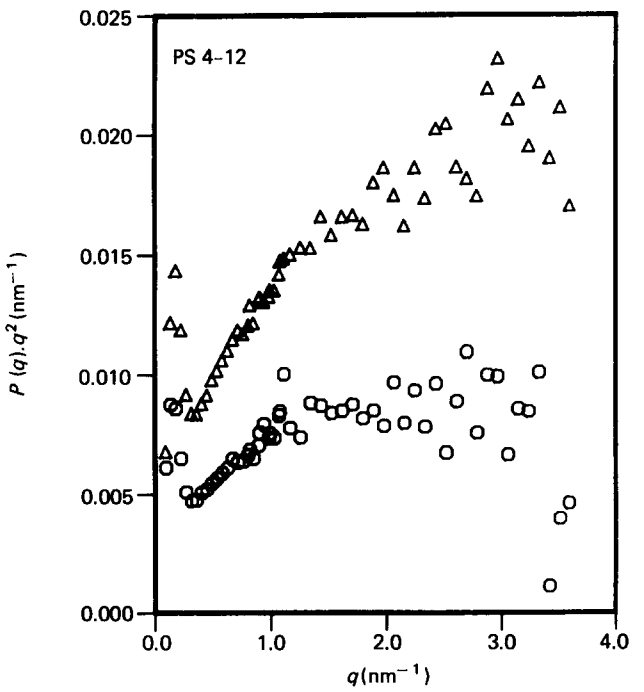

Figure 4 PS 4–12 in toluene-d_8 at $T = 20°C$; Kratky-plots of the scattering curves at c_1 (○) and c_4(△)

However, the finite rigidity of the chains should influence the particle scattering factor of star molecules in a similar manner as observed for linear chains[8]. Therefore, the increasing asymptote of the particle scattering factor in the Kratky-plot may qualitatively be interpreted, at least in part, in terms of the arm chain stiffness.

INFLUENCE OF SOLVENT ON THE SCATTERING CURVES

With the same samples used for the scattering experiments under θ-conditions, we performed SANS measurements in the good solvent toluene-d_8 at 20°C. The scattering curves now exhibited a marked concentration dependence, as is shown for the two concentrations of sample PS 4–12 in *Figure 4*.

Two facts make a detailed interpretation of the data difficult: (i) a concentration dependence which is not the same over the whole q-range and which makes an extrapolation of the scattering curves towards zero concentration unreliable, and (ii) the lack of any theory.

We therefore confine ourselves to a brief qualitative discussion. *Figure 5* represents scattering curves of the respectively lowest concentration from the sample PS 4–12 both in toluene-d_8 and cyclohexane-d_{12}. Clearly the good solvent toluene enlarges the deviations from theory[2]. These deviations were already observed under θ-conditions, i.e. lowering in the u-range immediately beyond u_{max}, and a continuous increase in the high u-range. The interaction with the good solvent leads to an expansion of the molecules and therefore makes the arms stiffer. This further stretching of the arms contributes to the enlarged deviations from theory.

THE RIGID ROD-LIKE STAR MODEL

To construct highly symmetric rod-like stars, we used the face normals of the well known platonic bodies. $\langle S^2 \rangle$ and $P(q)$ were determined by calculating numerically the double sums:

$$\langle S^2 \rangle = 1/2N^2 \sum_i^N \sum_j^N \langle r_{ij}^2 \rangle \quad (5)$$

$$P(q) = 1/N^2 \sum_i^N \sum_j^N \langle \sin qr_{ij} \rangle / \langle qr_{ij} \rangle \quad (6)$$

where N is the number of scattering centres. If the angles between the arms at the star centre are known, these double sums can be calculated according to a procedure, which is represented in *Table 2* for $f = 12$. In this Table, the double sums for $P(q)$ and $\langle S^2 \rangle$ are analysed with respect to the angles which are shown in *Figure 6*.

Figure 7 is a representation of Kratky-plots of the rod-like stars, corresponding to all platonic bodies, i.e. $f = 4$, 6, 8, 12, 20 together with $f = 3$ and the linear rod ($f = 2$). Similar to behaviour in the Gaussian model but not until $f > 4$ a maximum occurs in the low u-range. This maximum value $[P(u)u^2]_{max}$ is 1.15 and lies at $u_{max} = 1.8$. The fact that both, u_{max} and $[P(u)u^2]_{max}$ are independent of f is connected with the behaviour of $\langle S^2 \rangle$ which is proportional to N^2 and again independent of f.

The scattering curves exhibit undulations with increasing maximum values instead of a plateau value which is observed in the case of the Gaussian star model[2]. This can be explained by the correlation between the directions of the arms and the resulting highly symmetric arrangement of the scattering centres.

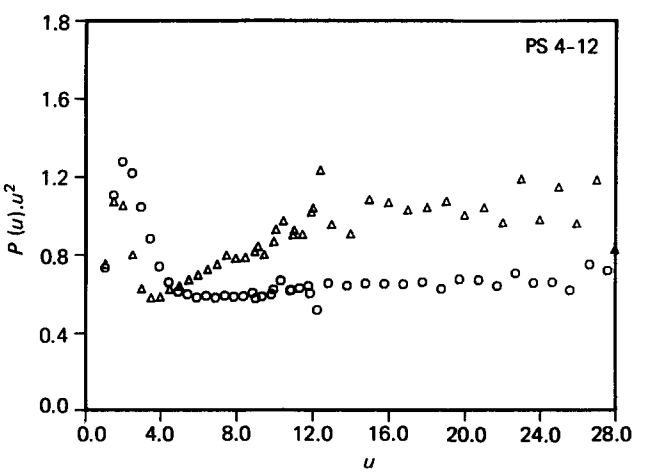

Figure 5 Kratky-plots of the sample PS 4–12; (○) in cyclohexane-d_{12} at $c = 0.00235\ g\,cm^{-3}$ with $u = q \times 10.97$ nm, (△) in toluene-d_8 at $c = 0.00415\ g\,cm^{-3}$ with $u = q \times 11.09$ nm

Table 2 Particle scattering $P(q)$ for a 12-arm rigid star molecule with rod-shaped arms and the scheme for calculation

Decomposition of the dodecahedron model

$$S(\beta)=\left(5\times 12\sum_{i=1}^{N}\sum_{j=1}^{N}\frac{\sin(q\cdot R)}{(q\cdot R)}\right)\Big/(N^2\times 12\times 5)$$

$$R=b(j^2-2ij\cos(64.4°)+i^2)^{1/2}$$

$$S(\gamma)=\left(5\times 12\sum_{i=1}^{N}\sum_{j=1}^{N}\frac{\sin(q\cdot R)}{(q\cdot R)}\right)\Big/(N^2\times 12\times 5)$$

$$R=b(j^2-2ij\cos(116.6°)+i^2)^{1/2}$$

$$S_1(\alpha)=\left(12\left(\sum_{i=1}^{N}2\frac{\sin(q\cdot i\cdot R)}{(q\cdot i\cdot R)}\right)+1\right)\Big/(24N+1)$$

$$S_2(\alpha)=12\left(\sum_{i=1}^{N}\sum_{j=1}^{N}\frac{\sin(q\cdot R)}{(q\cdot R)}\right)\Big/(N^2\times 12)$$

$$R=b(j^2-2ij\cos(0°)+i^2)^{1/2}$$

$$S_3(\alpha)=12\left(\sum_{i=1}^{N}\sum_{j=1}^{N}\frac{\sin(q\cdot R)}{(q\cdot R)}\right)\Big/(N^2\times 12)$$

$$R=b(j^2-2ij\cos(180°)+i^2)^{1/2}$$

$$P(q)=\frac{60N^2}{(12N)^2+1}(5S(\beta)+5S(\gamma))+\frac{12N^2}{(12N)^2+1}(S_2(\alpha)+S_3(\alpha))+\frac{1}{(12N)^2+1}(24N+1)S_1(\alpha)$$

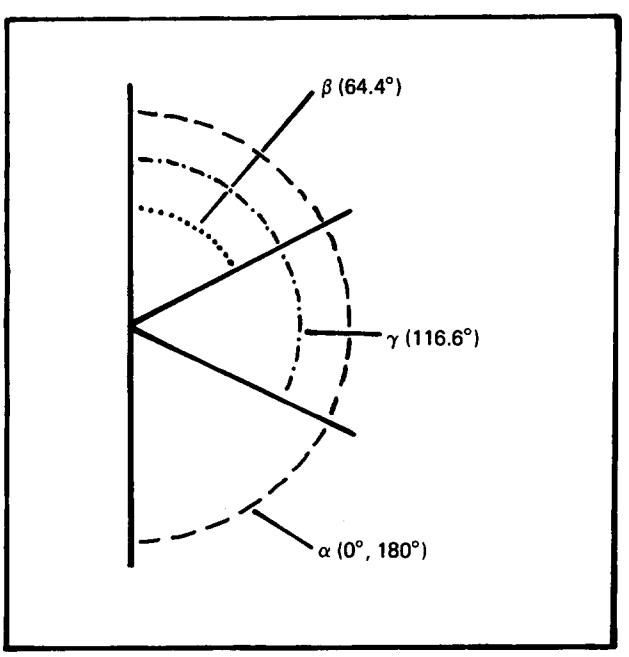

Figure 6 Angles between the rigid arms of the rod-like star model with $f=12$

A direct comparison of the two limiting models, i.e. the rod-like star model and Gaussian star model, is shown in *Figure 8*. In the u-range around u_{max}, the deviations from the Gaussian model are of the same quality as in the case of the SANS scattering curves shown in *Figures 2* and *3*. This behaviour appears unexpected at first sight because the rod-like star is not a reasonable model for a polymeric star chain as a whole. This point will be discussed further in the next section.

PARTICLE SCATTERING FACTORS OF SIMULATED R.I.S.-CHAINS

As mentioned above, two different methods were used to join together the arms to a regularly star-branched chain: (i) the combinatorial star (CS) and (ii) the star with a

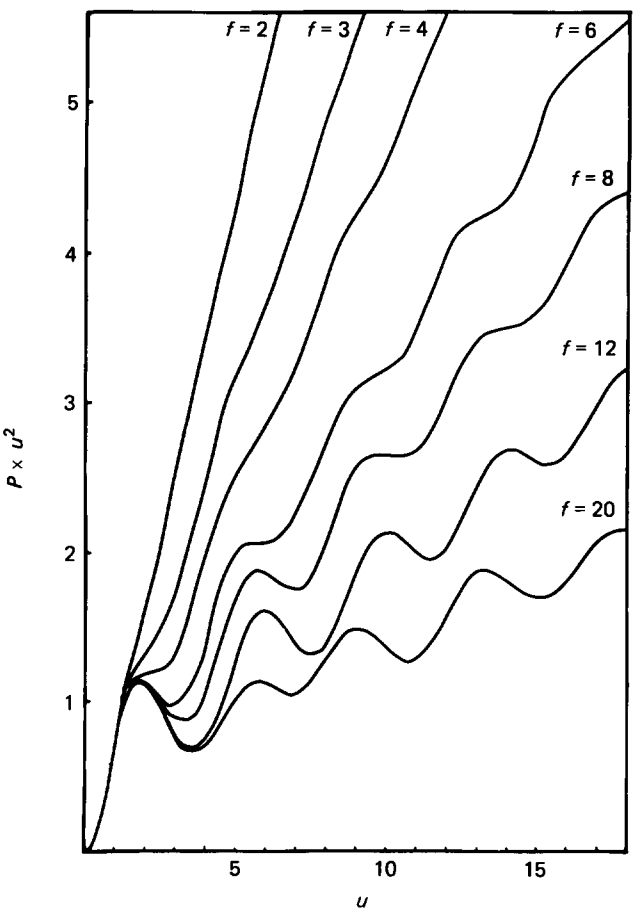

Figure 7 Kratky-plots of the particle scattering factors of the rod-like stars

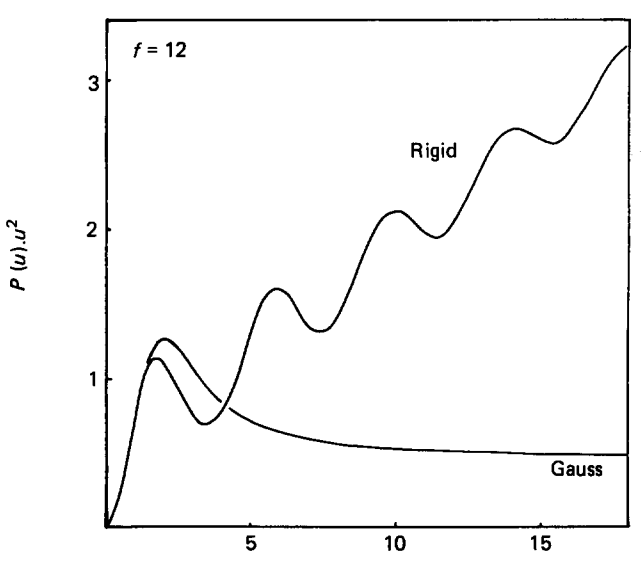

Figure 8 Comparison between the Kratky-plots of the two limiting models with $f=12$, i.e. the Gaussian and the rod-like star

specific centre (SPC). *Figure 9* represents particle scattering factors of a selection of different arm lengths, calculated with the CS-method, whereas *Figure 10* shows the corresponding curves for the SPC-method. The number of bonds is denoted by n_B. In both methods, the scattering curves are molecular weight dependent. Their deviations from the Gaussian star model are comparable with those which were observed with the SANS scattering curves of *Figures 2* and *3*. As in the case of the PS-star molecules, the continuously increasing parts at high u-values can be ascribed to the finite chain stiffness, which is inherent also to the r.i.s.-chains.

Direct comparison of the scattering curves from the CS-method with those from the SPC-method is now very instructive. Such a comparison was performed in the case of the smallest (*Figure 11*) and the largest (*Figure 12*) generated r.i.s.-star chains.

As can be seen from *Figure 11*, the particle scattering factors for very short star chains differ significantly from each other. Unlike the CS-method, the scattering curve from the SPC-method denoted by 'specific star centre' exhibits a second maximum. This situation is comparable with the undulations occurring with the scattering curves of the rod-like star model (*Figures 7* and *8*). The similarity between the scattering curves of short r.i.s. star chains from the SPC-method and

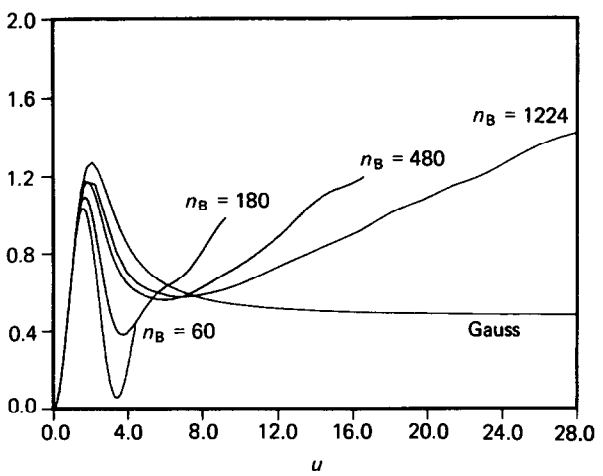

Figure 9 Kratky-plots of a selection of combinatorial r.i.s. star chains in comparison with the scattering curve of the Gaussian star model (Gauss)

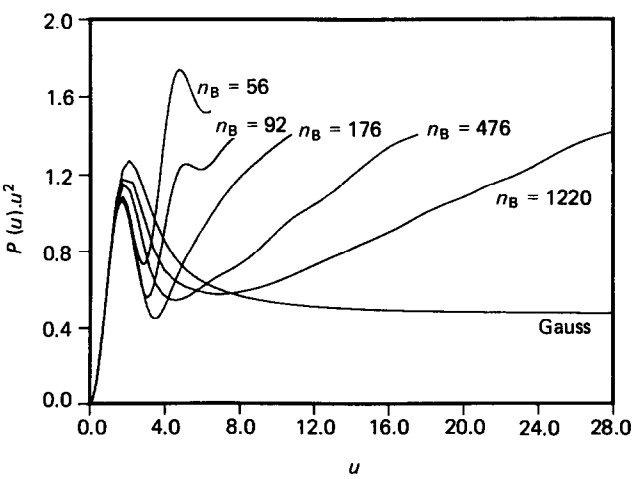

Figure 10 Kratky-plots of a selection of r.i.s. star chains with the specific star centre in comparison with the scattering curve of the Gaussian star model (Gauss)

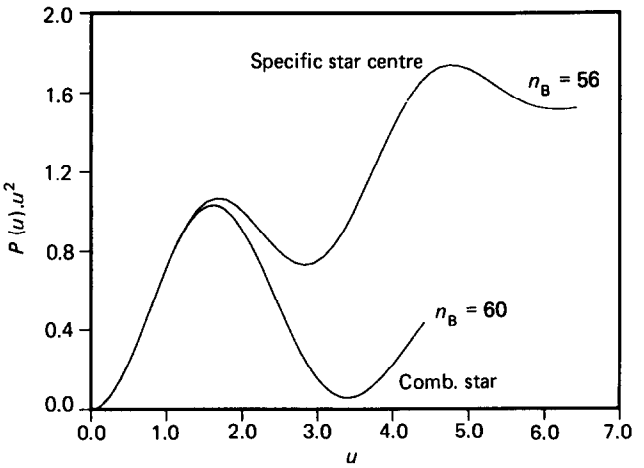

Figure 11 Comparison between the Kratky-plots of the smallest r.i.s. star chains simulated with the method using a specific star centre and with the combinatorial method

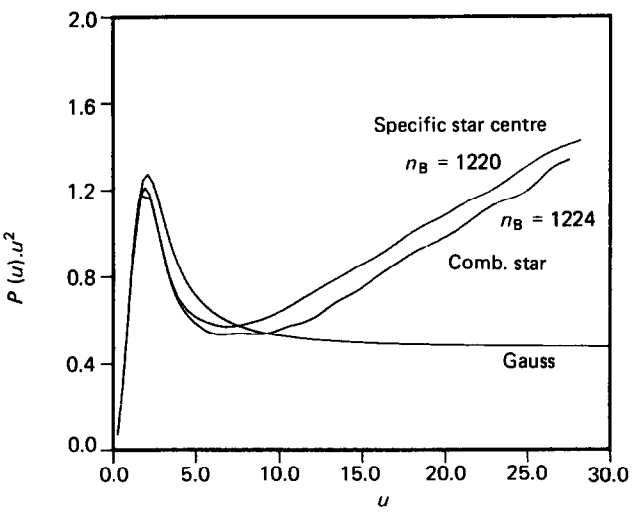

Figure 12 Comparison between the Kratky-plots of the longest r.i.s. star chains simulated with the method using a specific star centre and with the combinatorial method

of the rod-like star model supports the assumption that the rigid rod-like star can be used as a model for a star centre. The arms of the r.i.s. star chain are very short and the influence of the specific star centre on the scattering behaviour dominates. Due to this star centre, the correlation between the directions of the arms is marked and the segments are partially ordered.

On the other side, if the arms are very long (*Figure 12*), the differences between the scattering curves of the CS- and the SPC-methods diminishes. The mass fraction, for which the correlation between the directions of the arms plays an important role, decreases.

COMPARISON BETWEEN SANS RESULTS AND MONTE CARLO SIMULATIONS

To compare SANS results with scattering curves from r.i.s. star chains, we used the particle scattering curves of PS 9–12 at 28°C and PS 4–12 at 35°C in cyclohexane-d_{12}. As already mentioned, these scattering experiments were independent of concentration and therefore can be used for a comparison with Monte Carlo results.

Figure 13 is a representation of the scattering curve of PS 9–12 at concentration c_1, together with the scattering curves of the two largest simulated PM 12-arm star

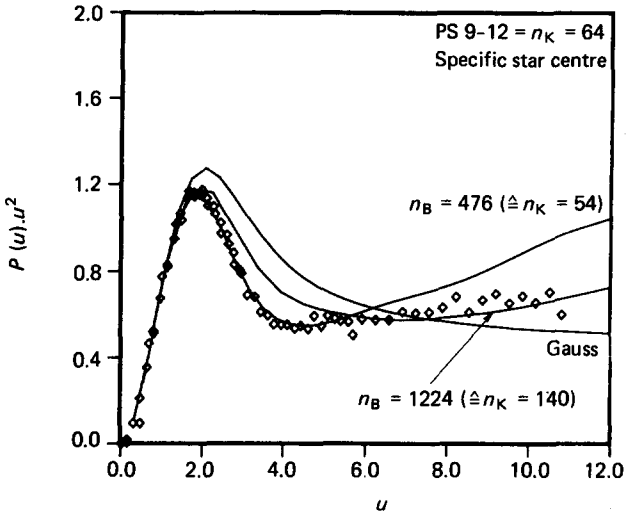

Figure 13 SANS scattering curve of PS 9–12 in cyclohexane-d_{12} at c_1 with $u = q \times 3.51$ nm (◇) in comparison with the particle scattering factors of the two longest simulated r.i.s. star chains with the specific star centre. The numbers denoted with n_K are numbers of statistical segments of the linear chains with the same chain length as the respective star chains

chains from the SPC-method. In addition the particle scattering factor of the Gaussian star model[2] was plotted. The maximum height of the SANS curves was fitted to one of the simulated chains yielding $\langle S^2 \rangle^{1/2} = 3.51$ nm, in fair agreement with the data of *Table 1*. In the range of $u < 6$, the simulated star chain with $n_B = 476$ provides an excellent description of the experimental scattering behaviour. Clearly the influence of the specific star centre on the particle scattering factor at this chain length is comparable with the influence of the star centre within the PS star molecules of the sample PS 9–12.

For a further investigation of the quality of the SPC- and CS-methods, we compared the same SANS scattering curve and the particle scattering factor of the r.i.s. chain with $n_B = 476$ (SPC-method) as in *Figure 3* now with the corresponding combinatorial star chain (*Figure 14*). In the range $u < 6$, the scattering curve of $n_B = 480$ (CS-method) exhibits significant deviations from the experimental data. The fact that the SPC-method provides a much better fit than the CS-method can be explained by the following argument: the sample PS 9–12 is of relatively low molecular weight and the influence of the star centre on the scattering behaviour cannot be neglected.

At first sight, the good agreement between the scattering curves of PS 9–12 and of the r.i.s. chain with $n_B = 476$ (SPC-method) appears somewhat arbitrary. However, an estimation of n_K, the number of Kuhn segments[8,12], of both the PS molecule and the PM chain, may lead to a better understanding of this fact. Within the worm-like chain model, n_K is determined by the following equations:

$$\langle S^2 \rangle = n_K l_K^2 / 6 \tag{7}$$

$$L = n_K l_K \tag{8}$$

where l_K is the Kuhn segment length and L the contour length of the whole chain. For PS 9–12 with a molecular weight of 5.5×10^4, n_K is calculated to be 64, whereas for the r.i.s. chain with 476 C–C bonds, n_K equals 54 (*Figure 13*). For this reason the agreement can be explained by the fact that both star types consist of a comparable number of statistical segments. However, one should keep in mind that this estimation of n_K can only be a rough approximation because it is based on the assumption that the Kuhn segment length of the star and the chain are identical.

To perform the same procedure with the sample PS 4–12, certain difficulties arise for the following reason; the molecular weight $M_w = 4.67 \times 10^4$ of PS 4–12 is relatively high. This high molecular weight corresponds to 543 Kuhn segments, i.e. 4.8×10^3 C–C bonds, so that the generation of a PM chain with such a high number of bonds would be too costly. We therefore increased the flexibility of the simulated chain, using the *a priori* probability weight matrix which corresponds to a carbon backbone chain with independent hindered rotation. Simulations with this matrix were already performed for linear chains[8]. The number of bonds which are necessary to produce a chain of about 540 Kuhn segments decreases to 1448 if the chain with independent hindered rotation is used.

PM 12-arm star chains were now generated both with the SPC-method ($n_B = 1448$) and with the CS-method ($n_B = 1452$). *Figure 15* represents the results of these

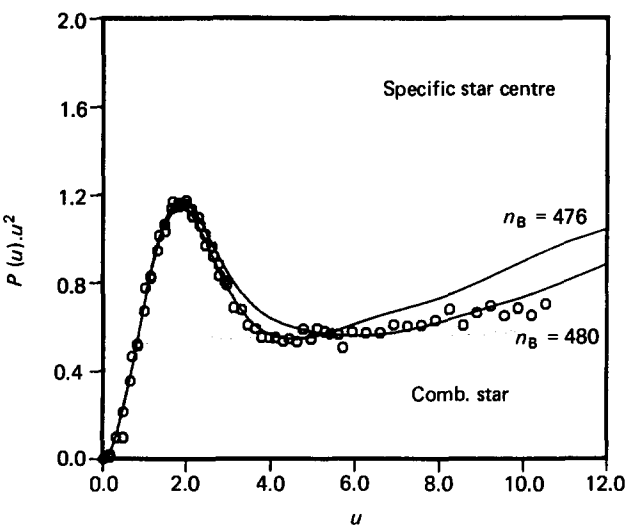

Figure 14 SANS scattering curve of PS 9–12 in cyclohexane-d_{12} at c_1 with $u = q \times 3.51$ nm (○) in comparison with the particle scattering factors of the simulated r.i.s. star chains with $n_B = 476$ (specific star centre) and with $n_B = 480$ (combinatorial star)

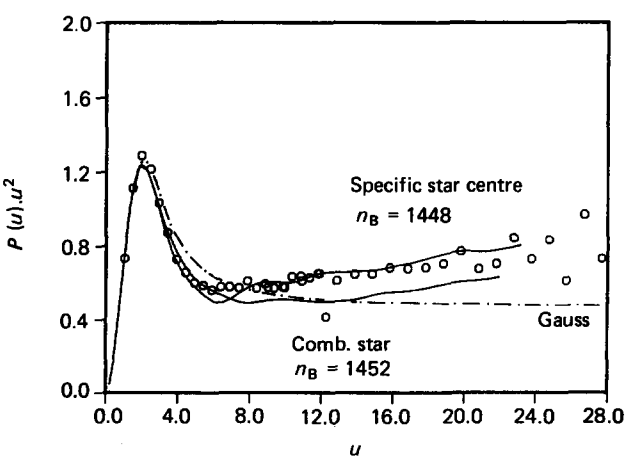

Figure 15 SANS scattering curve of PS 4–12 in cyclohexane-d_{12} at c_1 with $u = q \times 10.97$ nm (○) in comparison to the particle scattering factors of the simulated r.i.s. star chains with $n_B = 1448$ (specific star centre) and to $n_B = 1452$ (combinatorial star) using the *a priori* probability matrix corresponding to the independent hindered rotation

simulations together with the SANS scattering curve of sample PS 4–12 at concentration c_1. The SANS data were fitted to the maximum height of the scattering curve from the Gaussian model[2] using $\langle S^2 \rangle^{1/2} = 10.97$ nm. Though the scattering curves of both simulation methods exhibit only minor differences, the SPC curve is for $u < 25$ in a better agreement with the experiment than is the CS-curve. Therefore, even at a molecular weight range of $M_w \sim 5 \times 10^5$, the influence of a star centre on the scattering behaviour cannot be neglected.

The u-range, where good agreement is reached between the SPC-method and the PS-star molecules, is $0 < u < 6$ for PS 9–12 and $0 < u < 25$ for PS 4–12. In both cases this corresponds to $q < 2\,\text{nm}^{-1}$, which is the q-range where effects of chain microstructure are still negligible[8].

CONCLUSIONS

The experimentally determined particle scattering factors of PS 12-arm star molecules under θ-conditions exhibit significant deviations from the scattering behaviour expected for the Gaussian star model[2]. These deviations can be explained by two effects: (i) the chain stiffness, inherent to the arms of the star; (ii) the correlation between the initial directions of the arms, caused by fixed bond angles between the arms at the star centre.

At this point we wish once again to emphasize that the chosen temperature of 35°C is not exactly a θ-temperature for the star molecules. Nevertheless the slightly higher temperature had no detectable influence on the dimensions, and the whole scattering curve remained unchanged in the concentration range up to $8 \times 10^{-3}\,\text{g cm}^{-3}$. This represents typical behaviour of chains at the θ-temperature, and the experimental conditions may be thus considered as θ-conditions.

As pointed out in the preceding paper[1], chain stiffness should depend on the special position along the arms. However, an analytical description of chain stiffness within the star is not yet possible. On the other hand, further Monte Carlo simulations could develop the description of experimental scattering curves of PS 12-arm star molecules if the following improvements are introduced: (i) the use of the r.i.s. concept based on PS[13] and (ii) the use of an *a priori* probability weight matrix for PS, the elements of which depend on the position along the arm and which lead to a stiffening of the chain as the star centre is approached.

Finally it should be mentioned that the bigger cross-section of the PS chain should have a more pronounced self-exclusion effect than the modified methylene chain. It is well known that the self-exclusion has apparently no effect on the long range properties, e.g. R_g and R_h, for chains under θ-conditions. This fact results from a special, not yet fully understood balance between the attractive van der Waals force and the repulsive self-exclusion.

At shorter distances, on the other hand, the effect of the finite cross-section becomes effective and causes a weaker increase of the asymptote in the Kratky plot than is predicted by the Monte Carlo simulations. The agreement between measurement and simulation can be made better by introducing a finite cross-section which may be taken as an adjustable fitting parameter. We did not apply this procedure since we feel that the measurements should be carried out to the much larger values of $q = 15$ to $20\,\text{nm}^{-1}$. This region, however, is most difficult to study, because here the correction for incoherent neutron scattering is very large and causes very large errors.

ACKNOWLEDGEMENTS

We would like to thank the Institut Max von Laue–Paul Langevin for the use of their neutron scattering facilities. The help of the consultants at the Computation Centre of the University of Freiburg is kindly appreciated. The work was supported by the Deutsche Forschungsgemeinschaft within the scheme of SFB 60.

REFERENCES

1 Huber, K., Burchard, W., Bantle, S. and Fetters, L. J. *Polymer* 1987, **28**, 1990
2 Benoit, H. *J. Polym. Sci.* 1953, **11**, 561
3 Burchard, W. *Macromolecules* 1974, **7**, 841
4 Burchard, W. *Macromolecules* 1977, **10**, 919
5 Flory, P. J. 'Statistical Mechanics of Chain Molecules', Interscience Publishers, New York, USA (1969)
6 Zimm, B. H. and Stockmayer, W. H. *J. Chem. Phys.* 1949, **17**, 1301
7 Huber, K., Burchard, W. and Fetters, L. *Macromolecules* 1984, **17**, 541
8 Huber, K., Burchard, W. and Bantle, S. *Polymer* 1987, **28**, 863
9 Khorramian, B. A. and Stivala, S. S. *Polymer* 1986, **27** (*Commun.*), 184
10 Berry, G. C. *J. Chem. Phys.* 1966, **44**, 4550
11 Burchard, W. *Adv. Polym. Sci.* 1983, **48**, 1
12 Kuhn, W. *Kolloid Z.* 1936, **76**, 258; 1939, **87**, 3
13 Yoon, D. Y., Sundararajan, P. R. and Flory, P. J. *Macromolecules* 1975, **8**, 776